Effect of La³⁺ Substitution at Bi-Site on Transport Properties of $Bi_{0.3-x}La_xPr_{0.3}Ca_{0.4}Mn_{0.1}Cr_{0.9}MnO_3$

Norazila Ibrahim[1]*, Nor Asmira Amaran[2], Zakiah Mohamed[3], Ahmad Kamal Yahya[4]

Faculty of Applied Sciences, Universiti Teknologi MARA, 40450 Shah Alam, Selangor, Malaysia
*Corresponding author E-mail: noraz954@salam.uitm.edu.my

Abstract

Magnetic and electronic transport properties of $Bi_{0.3-x}La_xPr_{0.3}Ca_{0.4}Mn_{0.1}Cr_{0.9}O_3$ (0≤x≤0.2) manganites have been investigated by measurements of AC-susceptibility, resistivity and magnetoresistance. The samples were prepared using conventional solid-state synthesis method. Magnetic susceptibility versus temperature measurements showed all samples exhibit ferromagnetic to paramagnetic transition with Curie temperature, T_c enhanced from 111 K (x=0) to 174 K (x=0.2). Electrical resistivity measurements of the samples in zero field showed increase of metal-insulator (MI) transition temperature from 58 K(x=0) to 88 K(x=0.2). The increase in both T_c and T_{MI} indicates enhancement of double exchange (DE) interaction involving Mn^{3+} and Mn^{4+} ions as a result of weakening of the hybridization effect between Bi^{3+} $6s^2$ lone pair with O orbital due to La^{3+} substitution. La substitution in the Bi-based compound is suggested reduce MnO_6 octahedral distortion hence increasing delocalization of charge carriers. The observed variation in MR behavior due to La substitution indicates the substitution influence the MR mechanism of extrinsic and intrinsic behavior in $Bi_{0.3-x}La_xPr_{0.3}Ca_{0.4}Mn_{0.1}Cr_{0.9}O_3$.

Keywords:*A-Site substitution; Electrical conductivity; Magnetoresisatnce*

1. Introduction

Quite recently, a number of works have been focused on mixed valence manganites of the type $Ln_{1-x}D_xMnO_3$, where Ln represents trivalent rare earth ions such as La, Pr, Nd, Eu , Y and D represents alkaline ions such as Ca, Sr, Pb, Ba due to its unique physical properties such as the observation of colossal magnetoresistance effect (CMR) and transition of metal to insulator behavior which simultaneously occur at the same temperature region of ferromagnetic to paramagnetic transition [1-2]. The CMR effect, which is a phenomena related to the change of resistivity attributed to the improvement of charge carrier spin alignment induced by external magnetic field has generated considerable interest due to its potential application such as in spintronic based technologies [1-2]. The observed physical phenomena of metal-insulator transition and the MR effect can be understood by the double exhange (DE) mechanism which involves the interaction between pairs of Mn^{3+} and Mn^{4+} ions as proposed by Zener [3]. However other factors such as electron-phonon coupling arising from Jahn-Teller effect [4] have also been proposed to play a significant role on the observed variation of physical behavior which indicates that DE alone is not sufficient for a complete explanation of complex physical behaviours of mixed valence manganites.

Interestingly, for $Bi_{0.3}Pr_{0.3}Ca_{0.4}Mn_{0.9}Cr_{0.1}O_3$, the compound exhibits metal-insulator transition behavior at transition temperature, T_{MI} of 50 K indicating DE mechanism dominantly influences the resistivity behavior as a result of strong FM interaction between Mn^{3+}-O-Mn^{4+} and Cr^{3+}-O-Mn^{3+}[5]. The observed behavior was also suggested due to weakening of Bi-hybridization effect in $Bi_{0.3}Pr_{0.3}Ca_{0.4}Mn_{0.9}Cr_{0.1}O_3$ as a result of Cr substitution at Mn-site. The dominant effect of local distortion and hybridization between Bi-6s orbital with O-2p orbital which arise due to $6s^2$ lone pair

electrons [6] was suggested to be weakened due to enhancement of FM interaction which as a consequence may have reduced some type of blocking effect on electrons. In addition to that, the presence of antiferromagnetic, AFM superexchange interactions between Mn^{3+}-O-Mn^{3+}, Mn^{4+}-O-Mn^{4+}, Cr^{3+}-O-Cr^{3+} and Cr^{3+}-O-Mn^4 were also reported to favour magnetic inhomogeinity which was suggested to affect the observed MR behavior in $Bi_{0.3}Pr_{0.4}Ca_{0.6}Mn_{0.9}Cr_{0.1}O_3$. Obviously, more studies are required to better understand the special role of $6s^2$ lone pair electrons as well as the complex mechanism responsible for the observed MR effect. Interestingly, it was reported that La^{3+} substitution at Bi-site for $Bi_{0.6-x}La_xCa_{0.6}Mn_{0.9}O_3$ weakened charge ordered antiferromagnetic, COAFM phase and successfully induce ferromagnetic metallic, FMM phase which was suggested due to weakening of lattice distortion due to reduction of $6s^2$ lone pairs of Bi^{3+} [7].

In this work, the effects of La^{3+} substitution at Bi-site on electrical and magnetic properties of $Bi_{0.3-x}La_xPr_{0.4}Ca_{0.6}Mn_{0.9}Cr_{0.1}O_3$ were investigated. The substitution of La^{3+} was carried out to further understand the effects of local lattice distortion due to $6s^2$ lone pair on physical properties of doped bismuth-based manganites. Due to La^{3+} is isovalence with Bi^{3+} the Mn valence state is expected will not affected as a results of substitution. The ionic radius of La^{3+} almost similar to that Bi^{3+}, as such the factor which result to lattice distortion is expected due to special role of 6s lone pair. An analysis of the effects of La^{3+}on resistivity data for metallic and insulator regions based on electron-electron and electron-magnon scattering models and the variable-range hopping model, respectively, are also presented.

2. Methodology

$Bi_{0.3-x}La_xPr_{0.3}Ca_{0.4}Mn_{0.1}Cr_{0.9}O_3$ (x=0-0.2) samples were synthesized by the conventional solid-state synthesis method. Stoichio-
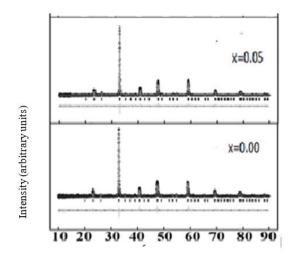
metric amounts of Bi_2O_3, Pr_6O_{11}, La_2O_3, $CaCO_3$, MnO_3 and Cr_2O_3 powders, all with high purity (>99.99 %) were weighed, mixed and ground thoroughly and then calcined at 850 ºC for 12 hours and then at 900 ºC for another 12 hours with intermediate grindings. The calcinated powders were then reground, pelletized and sintered at 1100 ºC for 24 hours with one intermediate grinding and finally the furnace was slow cooled to room temperature. The structural characterization of the obtained samples was carried out using X-ray powder diffraction (XRD) technique using a PANanalytical model Xpert PRO MPD diffractometer with CuK_α radiation for the range of 2θ= 15º-80º. The temperature variation of resistivity and magnetoresistance (MR) were carried out on circular shaped pellet using the standard four-point probe technique in a Janis model CCS 350ST cryostat, both under absence and presence of external magnetic fields of 0.8 T in the temperature range of 20 K – 300 K. AC susceptibility measurements were performed on powder samples in an AC susceptometer system under an average magnetic field of 0.5 Oesterd at frequency of 231 Hz in the temperature range of 15 K – 300 K and the real components were resolved using a Signal Recovery 7265 lock-in amplifier.

3. Results and Discussions

3.1. Structural Analysis

Fig. 1: Rietveld refinement of the XRD diffraction pattern along with diffraction pattern and the difference value between experimental and fitting plots for $Bi_{0.3x}La_xPr_{0.3}Ca_{0.4}Mn_{0.9}Cr_{0.1}O_3$ (x=0, x=0.05). Key: observed (cross), calculated (continuous line) and difference (continuous bottom line) and vertical tick marks above the difference plot show the Bragg peak positions

Figure 1 shows X-ray diffraction pattern of $Bi_{0.3-x}La_xPr_{0.3}Ca_{0.4}Mn_{0.9}Cr_{0.1}O_3$ (x =0, x= 0.05) where the characterization is performed using Cu-K$_\alpha$ radiation (λ=1.5406 Å) in the 15º-90º of 2θ range. The structure and cell parameter of all samples were analyzed using Rietveld refinement analysis which was performed using GSAS and VESTA program [8]. The refinement diffraction pattern and measured diffraction pattern of samples with x =0.00 and x = 0.05 are shown in **Figure 1** along with the difference in value between refinement and measured data at the bottom of both the diffraction patterns. The high quality of the refinement is confirmed by the value of χ^2 which suggests satisfactory fitting analysis. All the samples are found to exhibit single phase with diffraction peaks indexed based on orthorhombic structure with Pnma space group [5]. The final refinement values of lattice parameter, unit cell volume and bond angles are obtained and presented in Table1.The unit cell volume increased steadily with increase in La content indicates the substitution strongly

affects the strength of local lattice distortion, although the substitution involving smaller ionic radius of La^{+3}(1.16 Å) compared to Bi^{3+} (1.17Å) [7].

3.2. Magnetic properties

Figure 2 shows the variation of magnetic properties of $Bi_{0.3-x}La_xPr_{0.3}Ca_{0.4}Mn_{0.9}Cr_{0.10}O_3$ (x=0, x=0.05) samples as a result of La^{3+} substitution. All the samples were found to exhibit a ferromagnetic (FM) to paramagnetic (PM) phase transition at Curie temperature, T_C which is determined based on the minimum point of differentiation, $d\chi'/dT$ versus temperature curve [5]**.** Further increase in La doping level caused the T_C to increase from 111K (x=0) to 174 K (x=0.2) (**Table 1**). Substitution of La doping enhanced   FM phase in $Bi_{0.3-x}La_xPr_{0.3}Ca_{0.4}Mn_{0.9}Cr_{0.1}O_3$ ($0\leq x\leq0.2$) which resulted in the observed increased in T_C values. It is suggested that the introduction of La^{3+} for Bi^{3+} may have improved the Mn^{3+}/ Mn^{4+} spin alignment as the < Mn-O-Mn > increase due to substitution (Table 1). The reduction of MnO_6 lattice distortion may possibly contribute to the increase of < Mn-O-Mn > and subsequently the improvement of Mn^{3+}/ Mn^{4+} spin alignment as well as FM phase.
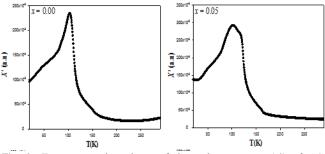

Fig. 2: Temperature dependence of the real component (χ') of AC susceptibility, χ' for $Bi_{0.3-x}La_xPr_{0.3}Ca_{0.4}Mn_{0.9}Cr_{0.10}O_3$ (0=0 and x=0.05)

3.3. Electrical properties

The temperature dependence of resistivity for $Bi_{0.3-x}La_xPr_{0.3}Ca_{0.4}Mn_{0.1}Cr_{0.9}O_3$ (x=0, x= 0.05) samples under zero and 0.8T magnetic field over the temperature range of 18 K-300 K are shown in **Figure 3**. At H=0 T, the x=0 sample showed metal-insulator (MI) transition (**Figure 3a**) with metal-insulator transition temperature, T_{MI} observed at 58 K. For x=0.05 of La doping (**Figure 3b**), the sample remained metallic with T_{MI} observed to slightly shift towards higher temperatures. For all other samples MI transition was also observed with increase in T_{MI} value from 61 K (x=0.05) to 88 K (x=0.2) with increasing La substitution (**Table 1**). Further, as shown in **Figure 3**, it is obvious that the application of low magnetic field decreased the resistivity of all the samples in the temperature region below T_{MI}. In addition, for all the samples T_{MI} slightly shifted to higher temperatures than that observed in the absence of magnetic field as shown in **Table 1.**
The resistivity of all the samples was observed to decrease with increasing La substitution indicating enhancement of the double exchange (DE) mechanism in the compound. It has been suggested that Bi^{3+} $6s^2$ lone pair can produce a local distortion due to hybridization between Bi- $6s^2$ orbital and O:2p orbital [6]. This hybridization would block the movement of e_g electron from Mn^{3+} to Mn^{4+} through Mn^{3+}-O-Mn^{4+} bridges. Further substitution of La at Bi sites, caused the local structural distortion to decrease as a result of decrease in Bi^{3+} concentration, resulting in delocalization of carriers. The change of resistivity behavior for La-substituted samples in the presence of magnetic field can be understood as follows. For the samples, the application of magnetic field caused the improvement in spin alignment within the grain hence increase delocalization of charge carrier which resulted in increase of DE and consequently resistivity decreased and T_{MI} slighlty shifts to high temperatures (Table 1).
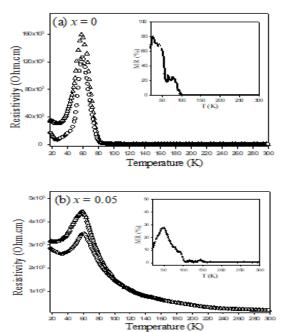
Fig. 3: Temperature dependence of resistivity under zero, 0 T (open triangles) and 0.8 T (open circles) magnetic field for $Bi_{0.3-x}La_xPr_{0.3}Ca_{0.4}Mn_{0.1}Cr_{0.9}O_3$ (a) x=0, (b) x=0.05 samples. Inset shows the temperature dependence of magnetoresistance, MR for the sample

The plots of MR versus temperature for La substituted samples are shown in the insets of **Figure 3a and Figure 3b**. The MR was calculated according to the equation MR(%) = (ρ(0,T)-ρ(H,T))/(ρ(0,T)) x 100%, where ρ(0) is the resistivity under zero magnetic field and ρ(H) is the resistivity under an applied field of 0.8 T. As shown in the inset of **Figure 3(a)**, the undoped sample exhibits a high intensity of MR peak which is 71%. Besides that, the intensity of MR peak was found to decrease from 27% for x = 0.05 to 19% for x = 0.1 (Table 1). Interestingly, both samples for x=0.15 and x=0.2 exhibit almost similar MR behavior in the low temperature region with maximum MR of around 20% at 20 K (Figure not shown). The observed high MR peak for x=0 at the vicinity of T_{MI} indicates the contribution of large intrinsic MR effect. It is related to the presence of enhanced delocalization of charge carriers as a result of improved spin alignment which resulted in the enhancement of DE [9,10]. However, the intrinsic MR effect may be weakened as the La concentration was further increased to x=0.1 as the intensity of the MR peak was reduced. Further substitution of La for x=0.15 and x=0.2 caused the disappearance of the MR peak. However, the MR value was found to gradually increase as temperature was decreased to below 100 K indicating that extrinsic MR mechanism increased as La concentration increased. This extrinsic MR arises due to spin-polarized tunneling or spin dependent scattering at the grain boundaries [9,10]. It is suggested that the application of low magnetic field may have enhanced polarization of the spin of the charge carriers in the field direction, thus increasing the number of carriers tunneling through the grain boundary and resulted in enhanced extrinsic MR effect.

Table 1: Lattice parameters, unit cell volume (V), metal-insulator transition temperature (T_{MI}) and Curie Temperature (T_c) for $Bi_{0.3-x}La_xPr_{0.3}Ca_{0.4}Mn_{0.9}Cr_{0.1}O_3$ (0≤x≤0.2)

Parameters	La^{3+} Content (x)				
	0	0.05	0.1	0.15	0.2
Lattice Parameters					
a (Å)	5.401(0)	5.408(0)	5.414(0)	5.419(0)	5.429(0)
b (Å)	5.441(0)	5.439(0)	5.436(0)	5.435(0)	5.434(0)
c (Å)	7.635(0)	7.644(0)	7.648(0)	7.652(0)	7.652(0)
V (Å^3)	224.34 (32)	224.91 (20)	225.15 (18)	225.43 (24)	225.80 (30)
χ^2	1.35	1.22	1.23	1.26	1.36

Bond angles(°)					
<Mn-O-Mn>	172.748 (1)	172.753 (1)	172.757 (0)	172.760 (1)	172.761 (1)
T_{MI} (at H=0T) (K)	58	61	62	68	88
T_{MI} (at H=0.8T) (K)	59	62	64	70	89
T_C	111	123	133	171	174

3.4. Conduction Mechanism in the Low-Temperature Region ($T< T_{MI}$)

In order to obtain better understanding of the nature of conduction mechanism in the low-temperature region ($T<T_{MI}$), the resistivity data both at H = 0T and H = 0.8T for all samples were fitted with an empirical equation as follows [5,7];

$$\rho = \rho_o + \rho_e T^{1/2} - \rho_s \ln T + \rho_p T^5 \tag{1}$$

In the equation, ρ_o represents the residual resistivity, which is related to scattering by impurities, defect, grain boundaries, or domain boundary effect or other temperature-independent scattering mechanisms, $\rho_e T^{1/2}$, is related with electron-electron Coulombic interaction while the term, $\rho_p T^5$, represents electron-phonon interaction. The term $\rho_s \ln T$ is resistivity attributed to Kondo-like spin-dependent scattering, which contributes to resistivity minimum behavior at low temperatures. It was found that the experimental data fitted well with the $\rho = \rho_o + \rho_e T^{1/2} - \rho_s \ln T + \rho_p T^5$ equation. Hence, it may be concluded that the resistivity in the ferromagnetic region below 87 K for all the samples may be attributed to the combination of electron-electron interaction, Kondo-like spin-dependent scattering and electron-phonon scattering effects. The best fit scattering parameters of ρ_o, ρ_e, ρ_s and ρ_p obtained are shown in the **Table 2.**

Table 2: Fitted parameters obtained from fitting experiment data in the metallic region to the equation $\rho = \rho_0 + \rho_e T^{1/2} - \rho_s \ln T + \rho_p T^5$ under zero magnetic field for $Bi_{0.3-x}La_xPr_{0.3}Ca_{0.4}Mn_{1-x}Cr_xO_3$ (x = 0.0 - 0.2)

Cr Content, x	ρ_0 (x10^3) (Ω-cm)	ρ_e (x10^3) (Ω-cm/$K^{1/2}$)	ρ_s (x10^4) (Ω-cm)	ρ_p (x10^{-5}) (Ω-cm/K^5)
0	116.913	103.96	10.069	1.0000
0.05	10.155	1.994	0.528	0.0906
0.1	13.209	2.000	0.616	0.0869
0.15	4.332	0.896	0.207	0.0025
0.2	3.919	0.838	0.216	0.0012

For undoped samples, the scattering effect is suggested to be stronger compared to other samples as all the fitting parameter show larger values compared to La doped samples. Interestingly, for x=0.05, La substitution seems to strongly reduce the scattering effect which may be related to increase in delocalization of charge carriers. The substitution is suggested to suppress the hybridization effect as concentration of Bi was reduced due to the substitution, thus a large drop in electrical resistivity at the low temperature region was observed. Further substitution of La at x=0.05-0.2, resulted in the scattering effect to be weakened as all the obtained values of scattering parameters decreased. Further, in the presence of applied magnetic field of 0.8 T, all fitting parameters decreased indicating magnetic field reduced scattering.

3.5. Conduction Mechanism at High Temperature: Variable Range Hopping Model and Small Polaron Model

In order to elucidate the nature of charge transport in $Bi_{0.3-x}La_xPr_{0.3}Ca_{0.4}Mn_{0.1}Cr_{0.9}O_3$ (0≤x≤0.2) in the temperature range of $T_{MI}<T<\theta_D/2$, the resistivity data of all samples was analyzed using the variable range hopping VRH model which is expressed by the following equation [5,7];

$$\rho = \rho_{om} \exp (T_{om} / T)^{1/4} \tag{2}$$

where T_{om} is the Mott's temperature which is related to the density of state at the Fermi level ($N(E_F)$) and hopping energy (E_h) as follows:

$$N(E_F) = 18\alpha^3 / k_B T_{om} \tag{3}$$

$$E_h(T) = 1/4 k_B (T)^{3/4} (T_{om})^{1/4} \tag{4}$$

where α is the localization length of 4.5 $\mathring{A}$ and k_B is the Boltzmann constant. To determine the value of T_{om} and E_h, the graph of $\ln(\rho)$ vs $1/T^{1/4}$ is plotted. The calculated values of hopping energy E_h, decreased from 146 meV ($x=0$) to 1.55 meV ($x=0.2$) while the calculated electronic density of state, $N(E_F)$ increased from $0.29 \times 10^{20} eV^{-1} cm^{-3}$ ($x=0$) to $148 \times 10^{20} eV^{-1} cm^{-3}$ ($x=0.2$). In addition, undoped sample show highest T_{om} of 780.0×10^5 K among the studied samples which reflects the strong lattice distortion of MnO_6 octahedral [11]. Small doping of La^{3+} ($x=0.05$) significantly suppressed the hybridization effect as well as reduced the lattice distortion of MnO_6 octahedral as T_{om} value is found to drastically decrease to 6.265×10^5 K. Further substitution of La^{3+} decreased T_{om} value indicating lattice distortion gradually decreased as hybridization between Bi lone pair and e_{gg} electrons of Mn^{3+} was reduced. The reduction of hopping energy, E_h (at T =120 K) indicates that the substitution enhanced the delocalization of charge carriers as reflected by the increased of value of $N(E_f)$, apart from possible reduction of Jahn-Teller effect. Hence, it is suggested the substitution significantly increased the probability of hopping process of charge carrier to their nearest neighbor potential difference as smaller energy is required for the process compared to unsubstituted sample. For the high temperature region, the resistivity data of sample $Bi_{0.3-x}La_xPr_{0.3}Ca_{0.4}Mn_{0.1}Cr_{0.9}O_3$ ($0 \leq x \leq 0.2$) is fitted by using small polaron hopping (SPH) model in the temperature region $T > \theta_{D/2}$. The respective equation for the model is represented by the following formula [5,7];

$$\rho(T) = \rho_o T \exp (E_a/k_B T) \tag{5}$$

where E_a is the activation energy, ρ_o is residual resistivity and k_B is the Boltzmann constant. The graph of $\ln(\rho/T)$ vs $1/T$ is plotted in order to determine the value of E_a. The unsubstituted sample show highest values of $E_a = 0.235$ meV compared to other samples which indicate larger amount of energy is required for hopping process of charge carrier. The result is supported by our suggestion on the dominant effect of the hybridization effect which results in some form of blocking effect leading to localization of charge carriers. For $x=0.05$, a drastic decrease of E_a to 0.064 meV is observed indicating substitution of La^{3+} strongly weakened the JT effect and reduced lattice distortion and enhanced the delocalization of charge carriers. When La^{3+} content x is increased, the E_a value continuously decreased to 0.047 meV ($x=0.2$) which indicates stronger suppression of the hybridization effect between Bi $6s^2$ lone pair and O orbital in the network.

4. Conclusion

In this paper, the magnetic and transport properties of $Bi_{0.3x}La_xPr_{0.3}Ca_{0.4}Mn_{0.1}Cr_{0.9}O_3$ ($0 \leq x \leq 0.2$) are presented. The substitution of La^{3+} caused increase in both T_c and $T_{MI\ indicating}$ improvement of ferromagnetic-metallic (FMM) phase. The observed behavior was due to enhancement of DE interaction between Mn^{3+}-O-Mn^{4+} as a result of the weakening of hybridization between Bi^{3+} $6s^2$ electron lone pairs with O orbitals which reduced MnO_6 octahedral distortion. The electrical resistivity in the metallic region for all samples were best fitted to electron-electron scattering, the Kondo-like effect and electron-phonon interaction models. The insulating region of resistivity in the temperature range $T_{MI} < T < T\theta_{D/2}$ can be explained based on the VRH model while in the range $T > T\theta_{D/2}$ involved the SPH model. The VRH and SPH models, respectively, revealed that the hopping and activation energy decreased as La^{3+} content increased due to the reduction in the distortion of MnO_6 octahedral. The observed variation in MR behavior due to La substitution indicates the substitution influence the MR mechanism of extrinsic and intrinsic behavior.

Acknowledgement

References

[1] N. Ibrahim and A. K. Yahya, "Inducement of Itinerant Electron Transport in Charge-Ordered Pr0.6Ca0.4MnO3 by Ba Doping", J. Supercond. Nov. Magn., vol 911, 2016.

[2] C.S. Xiong, F.F.Wei, et al, "Electrical properties and magnteelectric effect measurement in La0.7Ca0.2Sr0.1MnO3/xCoFe2O3 composites", Journal of Alloy and Compounds , vol 474, pp. 316-320, 2009.

[3] N.Ibrahim, A.K.Yahya, "Enhancement of extrinsic magnetoresistance behaviour in BiFeO3 doped La0.8Ag0.2MnO3 ceramic", Ceramics International , vol39, pp.S181-S184, 2013.

[4] R.Rozilah, N.Ibrahim, Z.Mohamed,A.k.Yahya, NawazishA.khan, M.Nasir Khan, "Inducement of ferromagnetic-metallic phase in intermediate charge -ordered Pr0.25Na0.25MnO3 manganite by K+ substitution", Phys B. Condens. Matter , vol 521 pp. 281-294, 2017.

[5] Kamlesh Yadav,H K Singh and G D Varma, "Effect of La-doping on magnetic properties of Bi0.6-xLaxCa0.4MnO3 (0.0≤ x≤0.6) perovskite manganites", Phys.Scripta, vol 85 , pp. 6 pages 045704, 2012.

[6] Ben Jazia Kharrat, S. Moussa, N. Moutiaa, K. Khirouni, W. Boujelben, "Structural, electrical and dielectric properties of Bi-doped Pr0.8-xBixSr0.2MnO3 manganite oxides prepared by sol-gel process", Journal of Alloys and Compounds, vol 724, pp. 389-399, 2017..

[7] N. Asmira, N. Ibrahim, Z. Mohamed and A.K. Yahya, "Effect of Cr3+ substitution at Mn-site on electrical and magnetic properties of charge ordered Bi0.3Pr0.3Ca0.4MnO3 manganites", Physica B, vol 544, pp.34-46, 2018.

[8] C. Zener, Interaction between the d-shells in the transition metals II. Ferromagnetic compounds of manganese with perovskite structure, Phys. Rev, vol 82, pp.403, 1951.

[9] A.J. Millis, P.B. Littlewood, B.I. Shraiman, "Double exchange alone does not explain the resistivity of La1-xSrxMnO3", J. Phys. Rev. Lett., vol 74, pp. 5144-5147, 1955.

[10] Tokura, Y. Tomioka, H. Kuwahara, A. Asamitsu, Y. Moritomo and M. Kasai, "Origins of colossal magnetoresistance in perovskite-type manganese oxides", Journal of Applied Physics, vol 79, pp.5288-5291, 1996.

[11] Jin, T.H. Tiefel, M. McCormack, R.A. Fastnacht, R. Ramesh and L.H. Chen, "Thousandfold change in resistivity in magnetoresistive La-Ca-Mn-O films", Science, vol 264, pp. 413-415, 1994.